AIP | Applied Physics Letters

Interplay of light transmission and catalytic exchange current in photoelectrochemical systems

Katherine T. Fountaine, Hans J. Lewerenz, and Harry A. Atwater

Citation: Applied Physics Letters **105**, 173901 (2014); doi: 10.1063/1.4900612
View online: http://dx.doi.org/10.1063/1.4900612
View Table of Contents: http://scitation.aip.org/content/aip/journal/apl/105/17?ver=pdfcov
Published by the AIP Publishing

Interplay of light transmission and catalytic exchange current in photoelectrochemical systems

Katherine T. Fountaine,[1,2,a)] Hans J. Lewerenz,[1] and Harry A. Atwater[1,3]
[1]*Joint Center for Artificial Photosynthesis, California Institute of Technology, 1200 E. California Blvd., Pasadena, California 91125, USA*
[2]*Department of Chemistry and Chemical Engineering, California Institute of Technology, 1200 E. California Blvd., Pasadena, California 91125, USA*
[3]*Department of Applied Physics and Materials Science, California Institute of Technology, 1200 E. California Blvd., Pasadena, California 91125, USA*

(Received 19 August 2014; accepted 15 October 2014; published online 27 October 2014)

We develop an analytic current-voltage expression for a variable junction photoelectrochemical (PEC) cell and use it to investigate and illustrate the influence of the optical and electrical properties of catalysts on the optoelectronic performance of PEC devices. Specifically, the model enables a simple, yet accurate accounting of nanostructured catalyst optical and electrical properties through incorporation of an optical transmission factor and active catalytic area factor. We demonstrate the utility of this model via the output power characteristics of an exemplary dual tandem solar cell with indium gallium phosphide and indium gallium arsenide absorbers with varying rhodium catalyst nanoparticle loading. The approach highlights the importance of considering interactions between independently optimized components for optimal PEC device design. © *2014 AIP Publishing LLC*. [http://dx.doi.org/10.1063/1.4900612]

The taxonomy of photoelectrochemically active systems distinguishes a variety of situations that are characterized by the nature of vectorial charge separation. The fundamental system, first proposed by Gerischer,[1,2] is based on the formation of a rectifying junction at the semiconductor–redox electrolyte contact that electronically resembles a Schottky contact[3] but is more conformal and optically transparent, and circumvents metal-induced gap states.[4,5] A second design involves a solid-state, buried p-n junction coupled to an electrocatalyst layer. Such structures have been prepared by *in-situ* surface transformations in electrochemical environments[6–9] showing considerable efficiency and notable stability. These results, obtained on technologically advanced semiconductors such as copper indium selenide ($CuInSe_2$) and indium phosphide (InP), have recently been complemented by the introduction of protection layers prepared by atomic layer deposition (ALD) to extend their stability.[10] As a consequence, a paradigm shift towards using technologically advanced semiconductors that enable high efficiencies in photoelectrochemical (PEC) energy conversion has occurred. In this context, the optimization of high-efficiency multijunction structures regarding charge transfer efficiency and stabilization is a particular challenge.

In this letter, we describe influential parameters for the efficiency of variable junction photoelectrochemical devices. Previously, we described the characteristic *J-V* behavior of a PEC half cell, a coupled electrocatalyst and photodiode,[11] using expressions for solid state photodiodes and Butler-Volmer[12,13] behavior of metallic electrocatalysts. Herein, we extend that analysis to a complete PEC device system and, additionally, consider the realistic optoelectronic consequences of nanostructured catalysts on the illuminated side of the device and propose strategies to minimize them.

As mentioned above, we previously determined the governing equation (Eq. (1)) for the *J-V* characteristic of a coupled photodiode-electrocatalyst (or a PEC half cell), $V_{halfcell}$, which has an overall voltage output that is the sum of the photodiode unit, V_{PV}, and the electrocatalytic overpotential, η_{cat}, where n_d is the diode ideality factor, j_L is the light-limited current density, $j_{0,PV}$ is the dark current of the photodiode, j is the operating current, n_e is the number of electrons associated with the electrochemical reaction, and j_0 is the catalyst exchange current density

$$V_{halfcell}(j) = V_{PV} + \eta_{cat}, \tag{1a}$$

$$V_{halfcell}(j) = \frac{n_d kT}{q}\ln\left(\frac{j_L - j}{j_{0,PV}} + 1\right) - \frac{2RT}{n_e F}\sinh^{-1}\left(\frac{j}{2j_{0,cat}}\right). \tag{1b}$$

In the present work, we elaborate on this equation to describe a realistic PEC device, containing a variable number of photodiode units, $V_{PV,i}$ and two catalysts, $\eta_{cat,a}$ and $\eta_{cat,c}$, for the anodic and cathodic reactions, respectively. Additionally, we include a series resistance term, V_{series}, to account for any non-ideal processes occurring throughout the device that result in series resistances (Eq. (2)). The sum of these voltages, V_{PEC}, is the photoelectrochemical device output voltage as a function of current density and must be greater than or equal to the thermodynamic potential of the desired reaction, E^0_{rxn}, in order for the reaction to proceed

$$V_{PEC}(j) = \sum_i V_{PV,i}(j) + \eta_{cat,a} + \eta_{cat,c} + V_{series}(j) \geq E^0_{rxn}. \tag{2}$$

For a simplistic analysis, the first and second terms of the right hand side of Eq. (1b) could be substituted for each

a)Author to whom correspondence should be addressed. Electronic mail: kfountai@caltech.edu.

of the photodiode terms, $V_{PV,i}$, and the anodic and cathodic catalyst terms, $\eta_{cat,a}$ and $\eta_{cat,c}$, respectively. However, these substitutions assume that the optoelectronic performance of the independent components are unaffected by their combination. For a half cell, this assumption is often valid because the catalyst resides on only one side of the half cell, and thus, the half cell can always be illuminated from the opposite side. Consequently, the catalyst layer can be optically thick without adversely affecting photodiode light absorption.

In contrast, a complete photoelectrochemical cell requires both an anodic and cathodic catalyst, which, in traditional device designs, resides on opposite sides of the cell; therefore, one of the catalysts is on the illuminated side of the device, reflecting and absorbing some of the incoming light. Thus, this catalyst layer reduces photodiode light absorption, and consequently, the light-limited current of the photodiode, j_L, with respect to its independent operation. To account for this non-unity transmission of light to the photodiode component, we introduce a transmission factor, f_T.

$$V_{PV,i}(j) = \frac{n_{d,i}kT}{q}\ln\left(\frac{j_{L,i}f_{T,i} - j}{j_{0,PV,i}} + 1\right). \tag{3}$$

Additionally, the catalyst layers in an optimized PEC device are unlikely to be conformal planar layers. Catalysts are often nanostructured to increase surface area and, thus, decrease overpotential; additionally, an illumination-side catalyst may be sparsely distributed to improve light transmission into the photodiode. Therefore, another factor, f_{SA}, is introduced to normalize the catalyst surface area to the planar device area, by modifying the catalytic exchange current density, $j_{0,cat}$

$$\eta_{cat,a/c}(j) = -\frac{2RT}{n_eF}\sinh^{-1}\left(\frac{j}{2j_{0,cat,a/c}f_{SA,a/c}}\right). \tag{4}$$

Substituting Eqs. (3) and (4) into Eq. (2) gives Eq. (5), the governing equation for the J-V characteristic of a realistic variable junction PEC device

$$\begin{aligned} V_{PEC}(j) = &\sum_i \frac{n_{d,i}kT}{q}\ln\left(\frac{j_{L,i}f_{T,i} - j}{j_{0,PV,i}} + 1\right) \\ &- \sum_{a,c}\frac{2RT}{n_eF}\sinh^{-1}\left(\frac{j}{2j_{0,cat,a/c}f_{SA,a/c}}\right) \\ &+ V_{series}(j) \geq E^0_{rxn}. \end{aligned} \tag{5}$$

Figure 1 exhibits the effect of modifying both factors, f_T and f_{SA}, on the J-V characteristic of a tandem ($i = 2$) system in terms of the normalized voltage (V/V_{OC}) and normalized current density (j/j_L). A decrease of catalyst surface area by a factor of 10 (blue to red line, $f_{SA} = 0.1$) results in a slower catalyst turn-on and a reduction in the output voltage of the tandem device at a given current. A 40% decrease in the light transmission through the catalyst (blue to green line, $f_T = 0.6$) directly results in a 40% decrease in the light-limited current, which consequently also causes a lower output voltage by the photodiode due to the logarithmic dependence of photodiode voltage on absorbed photocurrent.

Intuitively, complete transmission through the illumination-side catalyst ($f_T = 1$) and maximization of catalytic surface area (large f_{SA}) optimizes tandem device efficiency. However, in real

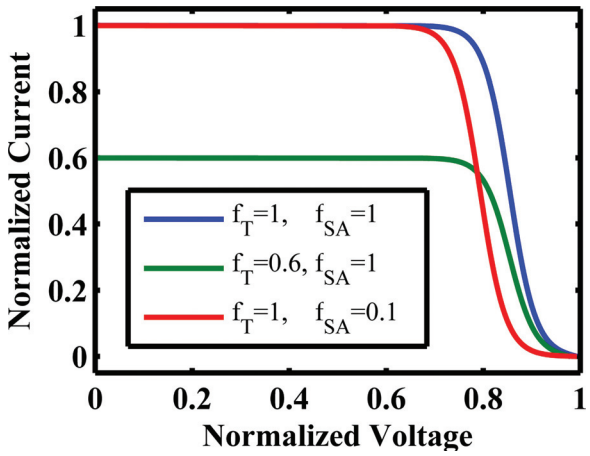

FIG. 1. Normalized current density vs. normalized voltage for (i) $f_T = 1$, $f_{SA} = 1$ (blue), (ii) $f_T = 0.6$, $f_{SA} = 1$ (green), and (iii) $f_T = 1$, $f_{SA} = 0.1$ (red). Eq. (3) was used with $j_L = 18.5\,\text{mA-cm}^{-2}$, $j_{0,PV1} = 10^{-19}\,\text{mA-cm}^{-2}$, $j_{0,PV2}$ $10^{-11}\,\text{mA-cm}^{-2}$, $j_{0,cat} = 0.1\,\text{mA-cm}^{-2}$, $n_e = 2$, $n_d = 1$, and $V_{series} = 0\,\text{V}$.

systems, these two factors cannot be independently optimized. Near unity transmission through a catalyst requires minimal usage of catalyst material, which subsequently implies low catalytic surface area.

To illustrate the interplay between these two factors, f_{SA} and f_T, we consider a tandem system consisting of indium gallium phosphide (InGaP) and indium gallium arsenide (InGaAs) photodiodes and rhodium (Rh) electrocatalysts that have been employed in water splitting half cells[14] with demonstrated high efficiency and stability for water-splitting[15] (Figure 2(a)). Optimization of this system involves careful tuning of catalyst deposition, typically experimentally performed via photoelectrodeposition, which generates an interfacial phosphate layer *in situ*.[14] To determine the values of f_T for this system, full-wave electromagnetic simulations of Rh hemispherical particles on a 10 nm interfacial layer of indium phosphate (InP_xO_y) and an optically thick InGaP substrate were performed using finite difference time domain methods. The Rh particle radius, r, and spacing, p, were varied. Table I summarizes the results of these simulations, where f_{T1} is the fraction of light transmitted through the catalyst up to the band edge of InGaP ($E_g = 1.78\,\text{eV}$) and f_{T2} is the fraction transmitted between the band edge of InGaP and InGaAs ($E_g = 1.26\,\text{eV}$). Transmission fractions are appropriately weighted to account for the power distribution of the AM1.5G spectrum. Constant values of p/r are used because this corresponds to equal aerial fill fraction and surface area enhancement factors, f_{SA}, for any value of particle radius. With some exceptions due to particle resonances, the transmission fractions, f_{Ti}, increase with decreasing f_{SA} (increasing p/r ratio), as expected.

Photoelectrodeposited Rh catalyst particles (Figure 2(a)) have a distribution of radii, the values for f_T are averaged over particle size for each value of f_{SA}. to approximate the optical response of this system. These f_T (f_{SA}) pairs are used with Eq. (5) to generate a model of the J-V characteristic for this tandem system to demonstrate the effects of varying nanostructured catalyst loading on the device performance.

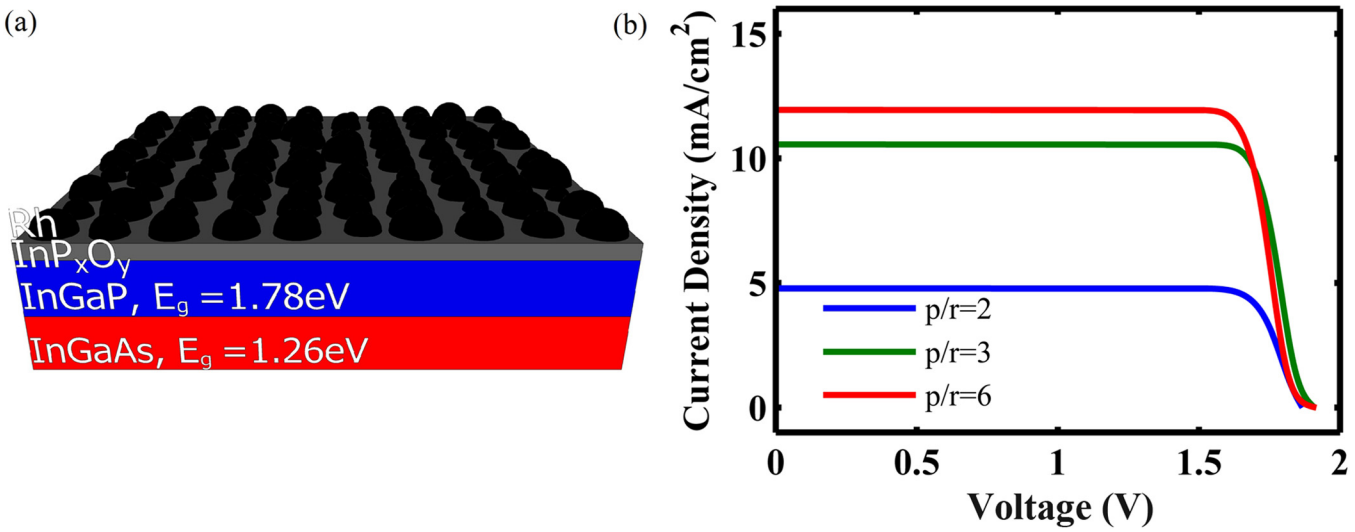

FIG. 2. (a) Schematic of modeled InGaAs/InGaP/interfacial InP_xO_y/Rh nanoparticles; (b) Current density vs. voltage for three values of particle spacing divided by particle radius (p/r = 2, 3, and 6). Eq. (3) was used with $j_L = 18.5\,mA\text{-}cm^{-2}$, $j_{0,PV1} = 10^{-19}\,mA\text{-}cm^{-2}$, $j_{0,PV2} = 10^{-11}\,mA\text{-}cm^{-2}$, $j_{0,cat} = 0.1\,mA\text{-}cm^{-2}$, $n_e = 2$, $n_d = 1$, and $V_{series} = 0\,V$.

TABLE I. Transmission factor values, $f_{T1}|f_{T2}$, for Rh hemispherical particles with varying radius, *r*, and spacing, *p*.

	r (nm)											
p/r (f_{SA})	10		25		50		100		150		250	
2 (1.57)	0.52	0.53	0.35	0.33	0.20	0.17	0.19	0.10	0.22	0.16	0.11	0.26
3 (0.70)	0.67	0.71	0.66	0.72	0.48	0.70	0.56	0.40	0.60	0.62	0.45	0.62
4 (0.39)	0.68	0.72	0.68	0.73	0.56	0.71	0.64	0.57	0.61	0.70	0.55	0.61
6 (0.17)	0.67	0.72	0.67	0.72	0.63	0.70	0.65	0.66	0.64	0.70	0.62	0.68

Figure 2(b) shows the *J-V* characteristic for a tandem InGaAs/InGaP/Rh electrochemical cell for the *p*/*r* values of 2 (blue), 3 (green), and 6 (red). For close-packed Rh hemispheres (p/r = 2, blue), the low transmission factor lowers the light-limited current density and, consequently, also decreases the photodiode voltage output. The *p*/r values of 3 and 6 illustrate the main trade-off in nanostructured catalyst design for a tandem electrochemical system. The moderate catalyst loading case (p/r = 3) has fairly good transmission, and, thus, short circuit current density, and a sharp catalytic turn-on. For the sparsely packed Rh particles (p/r = 6, green), the high transmission factor results in a large light-limited current density, but the catalytic turn-on is slower than the case of p/r = 3 due to low catalyst loading.

The optimum catalyst loading is dependent upon the specific device design and desired reaction. For the device design selected, the sparse catalyst loading is optimum because it maximizes the device current density and, despite the voltage penalty associated with decreasing the catalyst loading, the voltage supplied by the two photodiodes is still sufficient to drive the water splitting reaction ($E_{water\ splitting} = 1.23\,V$). In general, the device performance is more sensitive to changes in transmission than catalyst surface area because current depends linearly on the transmission factor and voltage depends approximately logarithmically on catalytic surface area ($\sinh^{-1}(x) \sim \ln(2x)$ for $x \gg 1$).

The authors are grateful to Matthias May, Thomas Hannappel, Frank Dimroth, and David Lackner for their contributions in the development of the tandem-electrocatalyst system that stimulated this research. This material is based upon work performed by the Joint Center for Artificial Photosynthesis, a DOE Energy Innovation Hub, supported through the Office of Science of the U.S. Department of Energy under Award No. DE-SC0004993. K.T.F. was supported by the National Science Foundation Graduate Research Fellowship under Grant No. DGE-1144469.

[1]H. Gerischer, J. Electroanal. Chem. **58**, 263 (1975).
[2]H. Gerischer, Surf. Sci. **18**, 97 (1969).
[3]H. J. Lewerenz, J. Electroanal. Chem. **356**, 121 (1993).
[4]V. Heine, Phys. Rev. A **138**, A1689 (1965).
[5]J. Tersoff, Phys. Rev. Lett. **52**, 465 (1984).
[6]S. Menezes, H. J. Lewerenz, and K. J. Bachmann, Nature **305**, 615 (1983).
[7]H. J. Lewerenz, in *Advances in Electrochemistry and Electrochemical Engineering*, edited by D. M. Kolb, R. C. Alkire, P. N. Ross, and J. Lipkowski (Wiley-VCH, 2010), Chap. 2, pp. 61–181.
[8]M. Noel and N. Suryanarayanan, J. Appl. Electrochem. **35**, 49 (2005).
[9]H. J. Lewerenz, C. Heine, K. Skorupska, N. Szabo, T. Hannappel, T. Vo-Dinh, S. A. Campbell, H. W. Klemm, and A. G. Munoz, Energy Environ. Sci. **3**, 748 (2010).
[10]S. Hu, M. R. Shaner, J. A. Beardslee, M. Lichterman, B. S. Brunschwig, and N. S. Lewis, Science **344**, 1005 (2014).
[11]M. R. Shaner, K. T. Fountaine, and H. J. Lewerenz, Appl. Phys. Lett. **103**, 143905 (2013).
[12]T. Erdey-Gruz and M. Volmer, Z. Phys. Chem. A **150**, 203 (1930).
[13]J. A. V. Butler, Trans. Faraday Soc. **19**, 729 (1924).
[14]A. G. Munoz, C. Heine, M. Lublow, H. W. Klemm, N. Szabo, T. Hannapel, and H. J. Lewerenz, ECS J. Solid State Sci. Technol. **2**, Q51 (2013).
[15]M. M. May, H. J. Lewerenz, F. Dimroth, D. Lackner, and T. Hannappel, "Efficient solar-to-hydrogen conversion by tailored *operando* interface transformation," Nature (submitted).